

Accepted Manuscript

---

This is an Accepted Manuscript of the following article:

T Gomes, Y Song, D A Brede, L Xie, K B Gutzkow, B Salbu, K E Tollefsen.  
Gamma radiation induces dose-dependent oxidative stress and  
transcriptional alterations in the freshwater crustacean *Daphnia magna*.  
*Science of the Total Environment*. Volume 628-629, 2018, pages 206-216,  
ISSN 0048-9697.

The article has been published in final form by Elsevier at

<http://dx.doi.org/10.1016/j.scitotenv.2018.02.039>

© 2018. This manuscript version is made available under the

CC-BY-NC-ND 4.0 license

<http://creativecommons.org/licenses/by-nc-nd/4.0/>

It is recommended to use the published version for citation.

---

1           **Gamma radiation induces dose-dependent oxidative stress and transcriptional**  
2                                   **alterations in the freshwater crustacean *Daphnia magna***

3 Tânia Gomes<sup>1,2\*</sup>, You Song<sup>1,2</sup>, Dag A. Brede<sup>2,3</sup>, Li Xie<sup>1,2</sup>, Kristine B. Gutzkow<sup>4</sup>, Brit Salbu<sup>2,3</sup>,  
4 Knut Erik Tollefsen<sup>1,2,3</sup>

5  
6 <sup>1</sup>Norwegian Institute for Water Research (NIVA), Section of Ecotoxicology and Risk  
7 Assessment, Gaustadalléen 21, N-0349 OSLO, Norway

8 <sup>2</sup>Centre for Environmental Radioactivity, Norwegian University of Life Sciences (NMBU),  
9 Post box 5003, N-1432 Ås, Norway

10 <sup>3</sup>Faculty of Environmental Science and Nature Resource Management, Norwegian University  
11 of Life Sciences (NMBU), Post box 5003, N-1432 Ås, Norway

12 <sup>4</sup>Department of Molecular Biology, Norwegian Institute of Public Health, Oslo 0403, Norway

13  
14  
15 \*Corresponding author: Tânia Gomes, Norwegian Institute for Water Research (NIVA),  
16 Section of Ecotoxicology and Risk Assessment, Gaustadalléen 21, N-0349 OSLO, Norway;  
17 Tel: (+47) 98215423, Fax: (+47) 221852 00; E-mail address: tania.gomes@niva.no.

18  
19  
20  
21  
22  
23  
24  
25

26 **Abstract**

27 Among aquatic organisms, invertebrate species such as the freshwater crustacean *Daphnia*  
28 *magna* are believed to be sensitive to gamma radiation, although information on responses at  
29 the individual, biochemical and molecular level is scarce. Following gamma radiation exposure,  
30 biological effects are attributed to the formation of free radicals, formation of reactive oxygen  
31 species (ROS) and subsequently oxidative damage to lipids, proteins and DNA in exposed  
32 organisms. Thus, in the present study, effects and modes of action (MoA) have been  
33 investigated in *D. magna* exposed to gamma radiation (dose rates: 0.41, 1.1, 4.3, 10.7, 42.9 and  
34 106 mGy/h) after short-term exposure (24 and 48 hrs). Several individual, cellular and  
35 molecular endpoints were addressed, such as ROS formation, lipid peroxidation, DNA damage  
36 and global transcriptional changes. The results showed that oxidative stress is one of the main  
37 toxic effects in gamma radiation exposed *D. magna*, mediated by the dose-dependent increase  
38 in ROS formation and consequently oxidative damage to lipids and DNA over time. Global  
39 transcriptional analysis verified oxidative stress as one of the main MoA of gamma radiation at  
40 high dose rates, and identified a number of additional MoAs that may be of toxicological  
41 relevance. The present study confirmed that acute exposure to gamma radiation caused a range  
42 of cellular and molecular effects in *D. magna* exposed to intermediate dose rates, and highlights  
43 the need for assessing effects at longer and more environmentally relevant exposure durations  
44 in future studies.

45

46 **Keywords:** Gamma radiation, *Daphnia magna*, oxidative stress, mode of action, gene  
47 expression.

48

49

50

## 51 **1. Introduction**

52 The increased use of nuclear technologies in the past decades has increased the concern on the  
53 impacts of man-made radionuclides in the environment, especially after the nuclear accident in  
54 Chernobyl in 1986 and more recently at Fukushima. In addition, other anthropogenic activities  
55 as routine discharges from nuclear power plants, nuclear weapons testing, mining, and nuclear  
56 waste from research facilities enhance the discharge of radionuclides into the aquatic  
57 environment thereby causing significant exposure of aquatic organisms (Unsear 2008).

58 Most radionuclides are gamma emitting, and gamma radiation can result in direct damage to  
59 biomolecules, such as double-strand breaks in genomic DNA (Ward, 1995), genotoxic DNA  
60 alterations (Parisot et al., 2015), chromosomal aberrations and mutations (Dallas et al., 2012),  
61 or indirectly damage macromolecules through the production of free radicals and reactive  
62 oxygen species (ROS) (Reisz et al., 2014). As a consequence, effects on a genetic and cellular  
63 level can result in significant impacts at the individual and population level, such as increased  
64 mortality and morbidity, reproduction impairment, shortening of life span and growth inhibition  
65 (Dallas et al., 2012; Fuller et al., 2015; Won et al., 2014). Although gamma radiation is known  
66 to induce toxicity in several aquatic invertebrates, knowledge of low dose effects on this diverse  
67 group of organisms is still limited compared to more extensively studied organisms such as fish  
68 and mammals. An overview of the effects of ionising radiation on aquatic invertebrates has  
69 already been carried out (Dallas et al., 2012; Fuller et al., 2015), highlighting the need for  
70 information regarding mechanisms of toxicity, early and sub-lethal effects in several groups of  
71 invertebrates, in for example the subphylum Crustacea. Crustaceans, such as the water flea  
72 *Daphnia magna*, have been identified as key models for the development of environmental  
73 radiation protection frameworks (ICRP, 2008).

74 *Daphnia magna* are small freshwater filter-feeding crustaceans that occupy a key position in  
75 the aquatic food web, not only as important phytoplankton grazers, but also as major food

76 sources for fish and invertebrate predators (Shaw et al., 2008). Daphnids are one of the most  
77 used invertebrate species in freshwater ecotoxicology and ecology mainly due to their  
78 comparatively short generation time, ease of culturing under laboratory conditions, capacity to  
79 reproduce through parthenogenesis and sensitivity to various environmental stressors  
80 (Watanabe et al., 2008). Accordingly, daphnids have been routinely used as standard model  
81 organisms in regulatory toxicity testing and detailed test guidelines have been developed  
82 (OECD, 2004, 2008; US EPA, 1996). Knowledge of the ecology, phylogeny, toxicology, and  
83 physiology of daphnia species in combination with a fully sequenced genome (wfleabase.org)  
84 has enabled a high number of exposure studies with different stressors in this species. Recent  
85 development of genomic tools, such as genetic linkage maps, cDNA libraries, expressed  
86 sequence tags databases and microarrays, have further enhanced the understanding of  
87 environmental-induced modulation of gene functions that may give rise to effects of ecological  
88 relevance (Kim et al., 2015; Shaw et al., 2008; Watanabe et al., 2008).

89 Previous studies have shown that exposure to acute doses of gamma radiation can cause  
90 significant mortality (Fuma et al., 2003), cause reduction in mobility and growth in daphnids,  
91 as well as a decrease in carbon incorporation in connection to reduced activity, filtering and  
92 ingestion rates (Nascimento et al., 2015, 2016; Nascimento and Bradshaw, 2016). Chronic  
93 exposure to gamma radiation can negatively impact survival, growth (decrease in body mass  
94 and length), metabolic dynamics (reduced resistance to starvation, decrease in mean-life span,  
95 alterations in respiration rate and mitochondrial activity) and reproduction (reduction in  
96 fecundity, delay in brood release and reduction in brood size) in daphnids, effects that were  
97 aggravated in subsequent generations (Gilbin, 2008; Marshall, 1962, 1966; Parisot et al., 2015;  
98 Sarapultseva and Gorski, 2013; Sarapultseva et al., 2017). Radiation-induced genotoxicity after  
99 chronic exposure was also reported in *D. magna* in the form of significant DNA alterations and  
100 transmission to progeny across generations (Parisot et al., 2015).

101 One of the most well-known toxic mechanisms of gamma radiation is the generation of ROS  
102 (e.g. superoxide radicals, hydroxyl radicals and hydrogen peroxide), either through direct  
103 interaction with the water in cells (formation of free radicals, recombination of radicals) or  
104 indirectly by the generation of secondary ROS by subsequent chemical cascades. The  
105 production of these radicals in excess can overwhelm the antioxidant capacity of cells and lead  
106 to oxidative stress due to oxidization of cellular components, instigating cell damage and other  
107 deleterious effects (Reisz et al., 2014). Some of the most common examples of biochemical and  
108 physiological damages associated with oxidative stress are lipid peroxidation (LPO) (formation  
109 of malonaldehyde-like species and 4-hydroxyalkenals), protein oxidation (e.g. carbonylation  
110 and cysteine oxidation) and DNA damage (e.g. single and double-strand breaks, 8-  
111 hydroxydeoxyguanosine and other oxidized bases), that have been described as some of the  
112 mechanisms involved in the damage caused by gamma radiation (Dallas et al., 2012; Fuller et  
113 al., 2015; Reisz et al., 2014). Even though it is well documented that gamma radiation can cause  
114 oxidative stress responses in several aquatic organisms (Dallas et al., 2012; Fuller et al., 2015;  
115 Won et al., 2014), detailed knowledge about the mode of action (MoA) of gamma radiation and  
116 linkage to phenotypical effects in crustaceans are still limited. Thus, acute toxicity of gamma  
117 radiation-induced oxidative stress was examined in *D. magna* by focusing on ROS formation,  
118 lipid peroxidation and DNA damage. In addition, alterations in the global gene expression were  
119 investigated to identify potential MoAs of gamma radiation in *D. magna*.

120

## 121 **2. Material and Methods**

### 122 **2.1. Test Organism**

123 *Daphnia magna* used in this study have been maintained in the NIVA laboratory for more than  
124 20 years (DHI strain NIVA, Oslo, Norway). *Daphnia magna* was cultured in EPA moderately  
125 hard media (MHRW, 96.0 mg/L NaHCO<sub>3</sub>, 60.0 mg/L CaSO<sub>4</sub>·2H<sub>2</sub>O, 60.0 mg/L MgSO<sub>4</sub>, 4.0

126 mg/L KCl, pH 7.2), which was renewed twice a week. Daphnids were fed daily with a  
127 suspension of the unicellular algae *Pseudokirchneriella subcapitata* and supplemented by an  
128 amount of dried baker's yeast (20 mg/mL). Cultures were kept in a climate room with light  
129 conditions set to 16:8 hr light: dark photoperiod and temperature  $20 \pm 1^\circ\text{C}$ , according to the  
130 OECD 202 guidelines (OECD, 2004). Under these conditions, female daphnids reproduce by  
131 parthenogenesis every three days. All cultures and exposures were initiated using third to fifth  
132 brood neonates aged <24 h old.

133

## 134 **2.2. Gamma radiation exposure**

135 Gamma radiation exposures were conducted at the FIGARO  $^{60}\text{Co}$  facility at the Norwegian  
136 University of Life Sciences (NMBU, Ås, Norway). *D. magna* neonates (<24h old) were  
137 exposed for 24 and 48 hrs to external gamma radiation under controlled climate conditions in  
138 accordance with the OECD 202 guidelines (OECD, 2004), with slight modifications to  
139 accommodate the experimental conditions used in this study. Neonates were exposed in 24-  
140 well plates (Falcon<sup>TM</sup>, Oslo, Norway) to 7 different gamma dose rates varying from 0.41 to  
141 106 mGy/h (see Supplementary Table A1 for more information on dose rates and total doses),  
142 along with a control placed behind lead shielding in the same room (background radiation).  
143 Experiments were conducted at the same temperature as that used for maintenance of *D. magna*  
144 cultures and in the dark, and exposure conditions as temperature, pH and dissolved oxygen were  
145 monitored for each dose rate throughout exposure. Immobilization and moulting frequency  
146 were recorded at 24 and 48 hrs. Due to relatively large sample size required for some of the  
147 parameters analysed, exposed daphnids were obtained across different experiments spaced in  
148 time, but subjected to the same experimental conditions. Three to six replicate plates were used  
149 for each endpoint, each plate with 10-12 daphnids depending on endpoint (see Supplementary  
150 Table A1 for more information on replication used). Field dosimetry (air kerma rates measured

151 with an ionization chamber) was traceable to the Norwegian Secondary Standard Dosimetry  
152 Laboratory (Norwegian Radiation Protection Authority, NRPA, Oslo, Norway) (Bjerke and  
153 Hetland, 2014). Dose rates to water in the centre of microplate wells (front row) were estimated  
154 according to Bjerke and Hetland (2014) and used as a proxy for the dose rates to exposed *D.*  
155 *magna*. Actual air kerma rates were measured using an Optically Stimulated Luminescence  
156 (OSL) based nanoDots dosimetry (Landauer) by positioning the nanoDots at the front of the  
157 microplates without use of build-up caps. Air kerma dose rates were calculated applying a  
158 conversion factor suggested by Hansen and Hetland (2015). Total doses were calculated from  
159 measured dose rates (mGy/h), multiplied by total exposure time (Supplementary Table A2).

160

### 161 **2.3. ROS formation**

162 Intracellular ROS production in *D. magna* exposed to gamma radiation was determined *in vivo*  
163 as described by Ma et al. (2012) and Xie et al. (2007) using the probes 2',7'-  
164 dichlorodihydrofluorescein diacetate (H<sub>2</sub>DCFDA, Invitrogen, Molecular Probes Inc., Eugene,  
165 OR, USA) and dihydrorhodamine 123 (DHR 123, Invitrogen, Molecular Probes Inc., Eugene,  
166 OR, USA), and adapted to the experimental conditions used in this study. Stock solutions of 20  
167 mM H<sub>2</sub>DCFDA and 5 mM DHR 123 were prepared in DMSO and kept at -20°C prior to use.  
168 On the day of the analysis, H<sub>2</sub>DCFDA and DHR123 stock solutions were diluted in MHRW to  
169 a final working solution of 2 mM. After 24h and 48 hrs exposure to gamma radiation, daphnids  
170 were collected and transferred in 200 µL MHRW to a 96-well black microplate (Corning  
171 Costar, Cambridge, MA, USA), with 10-12 replicates per dose rate. Only surviving daphnids  
172 were used for the determination of ROS. For each dose rate, 5 µL of either H<sub>2</sub>DCFDA or DHR  
173 123 working solutions were immediately added to each well (50 µM final concentration) and  
174 the microplate covered with aluminium foil and incubated for 6 hrs under laboratory conditions.  
175 Fluorescence was recorded hourly on a microplate fluorescent reader Fluoroskan Ascent 2.5,



176 ThermoFisher Scientific, USA) with excitation/emission of 485/538 nm. Natural fluorescence  
177 of irradiated MHRW in combination with the probes (without presence of daphnids) for each  
178 dose rate was also analysed and the resulting fluorescence subtracted. The relative fluorescence  
179 obtained for both probes at each dose rate was expressed as fold induction comparative to the  
180 control. Two independent experiments were run to determine the formation of ROS in daphnia  
181 exposed to gamma radiation. Hydrogen peroxide (H<sub>2</sub>O<sub>2</sub>, CAS number: 7722-84-1, purity  
182  $\geq 30\%$ ) was used as positive control for both probes following the same procedure, in  
183 concentrations ranging from 1–50  $\mu\text{M}$ .

184

#### 185 **2.4. Lipid peroxidation**

186 Lipid peroxidation (LPO) was assessed by determining malondialdehyde (MDA) and 4-  
187 hydroxyalkenals (4-HNE) concentrations upon decomposition by polyunsaturated fatty acid  
188 peroxides, following the method described by Erdelmeier et al. (1998). Briefly, after 24 and 48  
189 hrs exposure to gamma radiation, 5 to 6 groups of 36 daphnids were pooled, frozen in liquid  
190 nitrogen and stored at  $-80^{\circ}\text{C}$  until further analysis. Pooled daphnids were homogenized using a  
191 Precellys tissue Homogenizer (Bertin Technologies, Montigny-le-Bretonneux, France) in 0.02  
192 M Tris-HCl containing 0.5 M BHT (pH 7.4) at  $4^{\circ}\text{C}$ . The resulting homogenate was centrifuged  
193 at 3000 g for 10 minutes at  $4^{\circ}\text{C}$  and the supernatant used for protein determination and LPO  
194 analysis. LPO analysis was based on the reaction of two moles of N-methyl-2-phenylindole  
195 (3:1 mixture of acetonitrile/methanol), a chromogenic reagent, with one mole of either MDA  
196 or 4-HNE under acidic conditions (methanesulfonic acid) at  $45^{\circ}\text{C}$  for 60 min to yield a stable  
197 chromophore with maximum absorbance at 586 nm. Malondialdehyde bis-(1,1,3,3-  
198 tetrametoxopropane) was used as a standard. Protein content was determined using the Bradford  
199 method (Bradford, 1976) with Immunoglobulin G (IgG) as a standard. Lipid peroxidation was  
200 expressed as fold induction comparative to the control.

201

## 202 **2.5. Comet Assay**

203 The alkaline Comet Assay was performed on haemolymph cells from exposed daphnids,  
204 according to the method by Pellegrini et al. (2014) and adapted to the high throughput single cell  
205 gel electrophoresis described in Gutzkow et al. (2013). After 24 and 48 hrs exposure, pools of  
206 24 daphnids (3 biological replicates) were placed in PBS buffer without  $\text{Ca}^{2+}/\text{Mg}^{2+}$  (pH 7.4)  
207 and haemolymph cells extracted by mechanical dissociation using a metal grinder. After  
208 haemolymph extraction, the buffer containing the cells was filtered using a 55  $\mu\text{M}$  nylon mesh  
209 and the resulting cell suspension centrifuged at 300 *g* for 5 minutes (4°C). The pellet was gently  
210 resuspended in PBS buffer without  $\text{Ca}^{2+}/\text{Mg}^{2+}$  (pH 7.4) and the final cell suspension adjusted  
211 to  $1 \times 10^6$  cells/mL. Cell viability was checked using the trypan blue exclusion assay. Cells were  
212 resuspended in 1:10 0.75 % low melting point agarose at 37 °C and triplicates (3×4  $\mu\text{L}$ ) from  
213 each biological replicate were immediately applied on a cold GelBond® film. Lysis was  
214 performed overnight in lysis buffer (2.5 M NaCl, 0.1 M  $\text{Na}_2\text{EDTA}$ , 0.01 M Tris, 0.2 M NaOH,  
215 0.034 M N-laurylsarcosine, 10 % DMSO, 1 % Triton X-100, pH 10) at 4°C. For unwinding,  
216 films were immersed in cold electrophoresis solution (0.3 M NaOH, 0.001 M  $\text{Na}_2\text{EDTA}$ , pH >  
217 13) for 40 min. Electrophoresis was carried out in cold, fresh electrophoresis solution for 20  
218 min at 8 °C, 25 V giving 0.8 V/cm across the platform, with circulation of electrophoresis  
219 solution. After electrophoresis, films were neutralized with neutralisation buffer (0.4 M Tris–  
220 HCl, pH 7.5) for 2×5 min, fixed in ethanol (>90 min in 96 % ethanol) and dried overnight.  
221 Films were stained with SYBR® Gold Nucleic Acid Gel Stain (Life Technologies, Paisley, UK)  
222 in TE-buffer (1 mM  $\text{Na}_2\text{EDTA}$ , 10 mM Tris–HCl, pH 8) before examination at a 20×  
223 magnification under an Olympus BX51 microscope (light source: Olympus BH2-RFL-T3,  
224 Olympus Optical Co., Ltd.; camera: A312f-VIS, BASLER, Ahrensburg, Germany). Fifty  
225 randomly chosen cells per replicate (150 cells per biological replicate, total 450 cells per dose

226 rate) were scored using the Comet IV analysis software (Perceptive Instruments Ltd., Bury St.  
227 Edmunds, UK). Tail intensity (% Tail DNA), defined as the percentage of DNA migrated from  
228 the head of the comet into the tail, was used as a measure of DNA damage induced by gamma  
229 radiation because it has been shown to be the most meaningful endpoint to assess genotoxicity  
230 (Kumaravel and Jha, 2006). The mean percentage (%) of DNA in the tail per biological replicate  
231 was calculated using the median values of % tail DNA from the 50 comets from each technical  
232 replicate. Treatment with hydrogen peroxide (H<sub>2</sub>O<sub>2</sub>, CAS number: 7722-84-1) was used as the  
233 positive control following the same procedure, in concentrations ranging from 1 to 10 μM.

234

## 235 **2.6. Microarray gene expression analysis**

236 After 24 hrs exposure to gamma radiation, six daphnids were pooled for each replicate (n=5),  
237 sampled in RNALater (Sigma-Aldrich) and stored at -80°C until use. Total RNA was isolated  
238 using the ZR Tissue & Insect RNA MicroPrep kit in combination with on-column DNase I  
239 treatment (Zymo Research Corp., Irvine, CA) as previously described (Song et al., 2016). The  
240 purity (260/280>1.8, yield > 100 ng) and integrity (clear RNA peaks, flat baselines) of RNA  
241 were assessed using Nanodrop ND-1000 (Nanodrop Technologies, Wilmington, DE) and  
242 Bioanalyzer (Agilent Technologies, Santa Clara, CA, USA), respectively.

243 Transcriptomic analysis was performed using Agilent custom 60,000-feature *D. magna*  
244 oligonucleotide microarrays and 50 ng input RNA according to Agilent's standard protocol  
245 "One-Color Microarray-Based Gene Expression Analysis, version 6.5", with modifications  
246 (Song et al., 2016). Raw microarray data (signal intensity) was extracted from scanned images  
247 using the Feature Extraction software v10.7 (Agilent), and data corrected for baseline variance  
248 (normexp method), inter-array variance (quantile method), filtered for low expression probes  
249 and technical replicate probes merged using the Bioconductor package LIMMA (Smyth, 2005)  
250 in the R statistical environment v3.1.2, as previously described (Jensen et al., 2016).

251 Differentially expressed genes (DEGs) were determined using LIMMA by contrasting gamma-  
252 exposed groups to the control ( $p < 0.05$ ). Gene ontology (GO) enrichment analysis was  
253 performed towards crustacean GO databases using a hypergeometric test ( $p < 0.05$ ) implemented  
254 in Cytoscape v3.1.1 (Smoot et al., 2011) via the Bingo plugin v2.4 (Maere et al., 2005). The *D.*  
255 *magna* DEGs were further mapped to *Drosophila melanogaster* orthologs in order to perform  
256 Reactome pathway enrichment analysis ( $p < 0.05$ ) using the Cytoscape plugin ClueGO v2.1.4  
257 (Bindea et al., 2009). Venn diagram analyses were performed using Venny  
258 (<http://bioinfogp.cnb.csic.es/tools/venny/>) and Sumo software package  
259 (<http://angiogenesis.dkfz.de/oncoexpress/software/sumo/>). No multiple testing corrections  
260 were performed to avoid loss of DEGs and GO/pathways that may potential have high relevance  
261 for gamma-induced stress response profiles (Song et al., 2014; 2016).

262

## 263 **2.7. Quantitative real-time PCR analysis**

264 A selection of 13 target genes considered relevant to potential MoAs of gamma radiation was  
265 further verified using quantitative real-time reverse transcription polymerase chain reaction  
266 (qRT-PCR) essentially as described by Song et al. (2016). The qRT-PCR analysis was conducted  
267 on a CFX384 Touch™ Real-Time PCR Detection System (Bio-Rad Laboratories, Oslo,  
268 Norway) using the same RNA as used in the microarray analysis ( $n=5$ ). Primers used for cDNA  
269 amplification were designed using the online software Primer3 v4.0.0 (<http://primer3.ut.ee/>)  
270 and purchased from Invitrogen™ (Carlsbad, California, USA) (Supplementary Table A3).  
271 Briefly, cDNA was made from total RNA (82.5 ng) using qScript™ cDNA SuperMix (Quanta  
272 BioSciences™, Gaithersburg, MD, USA), and amplified in a 20  $\mu$ l reaction (1 ng cDNA, 400  
273 nM forward/reverse primer and 15  $\mu$ l PerfeCTa® SYBR® Green FastMix® (Quanta  
274 BioSciences™)) using the Bio-Rad CFX384 platform (Bio-Rad Laboratories, Hercules, CA).  
275 Four biological replicates (each containing two technical replicates), no-reverse-transcriptase

276 (NRT) and no-template controls (NTC) were included in the amplification. Pooled cDNA  
277 (0.25–4 ng) was used to generate a standard curve for determination of amplification efficiency.  
278 The relative expression was calculated using the Pfaffl method (Pfaffl, 2001). Gene expression  
279 data for target genes was normalized to the geometric mean expression of three reference genes,  
280 beta actin ( $\beta$ -actin), cyclophilin (Cyp) and glyceraldehyde 3-phosphate dehydrogenase  
281 (Gadph), to compensate for any difference in initial RNA quantity and in reverse transcriptase  
282 efficiency. The normalized expression of each target gene was further normalized to the mean  
283 expression of the control.

284

## 285 **2.8. Statistical Analysis**

286 Statistical analyses were performed using XLStat2016® (Addinsoft, Paris, France) and  
287 GraphPad Prism 6 (GraphPad Software Inc., La Jolla, CA, USA). Data was tested for normality  
288 and homogeneity of variances using Shapiro-Wilk and Levene's tests, respectively, to check if  
289 all parameters satisfied the assumptions associated with parametric tests. Differences between  
290 dose rates and time of exposure were compared for ROS production, LPO and DNA damage  
291 data using a 2-way ANOVA followed by the post-hoc Tukey test. Gene expression results were  
292 analysed for significant differences between dose rates either with one-way analysis of variance  
293 (ANOVA) or Kruskal–Wallis One Way Analysis of Variance on Ranks. If significant, pairwise  
294 multiple comparison procedures were conducted, using the Tukey test or the Dunn's method.  
295 For qPCR data, outliers were removed using the ROUT test implemented in GraphPad. A  
296 Pearson correlation analysis was also performed between the mean relative gene expression  
297 values obtained by qPCR compared to mean relative gene expression values for the same genes  
298 from the microarray analysis for all exposure groups. Statistical significance was set at  $p < 0.05$   
299 for all statistical analyses.

300

### 301 **3. Results**

#### 302 **3.1. Effects on mortality and exposure parameters**

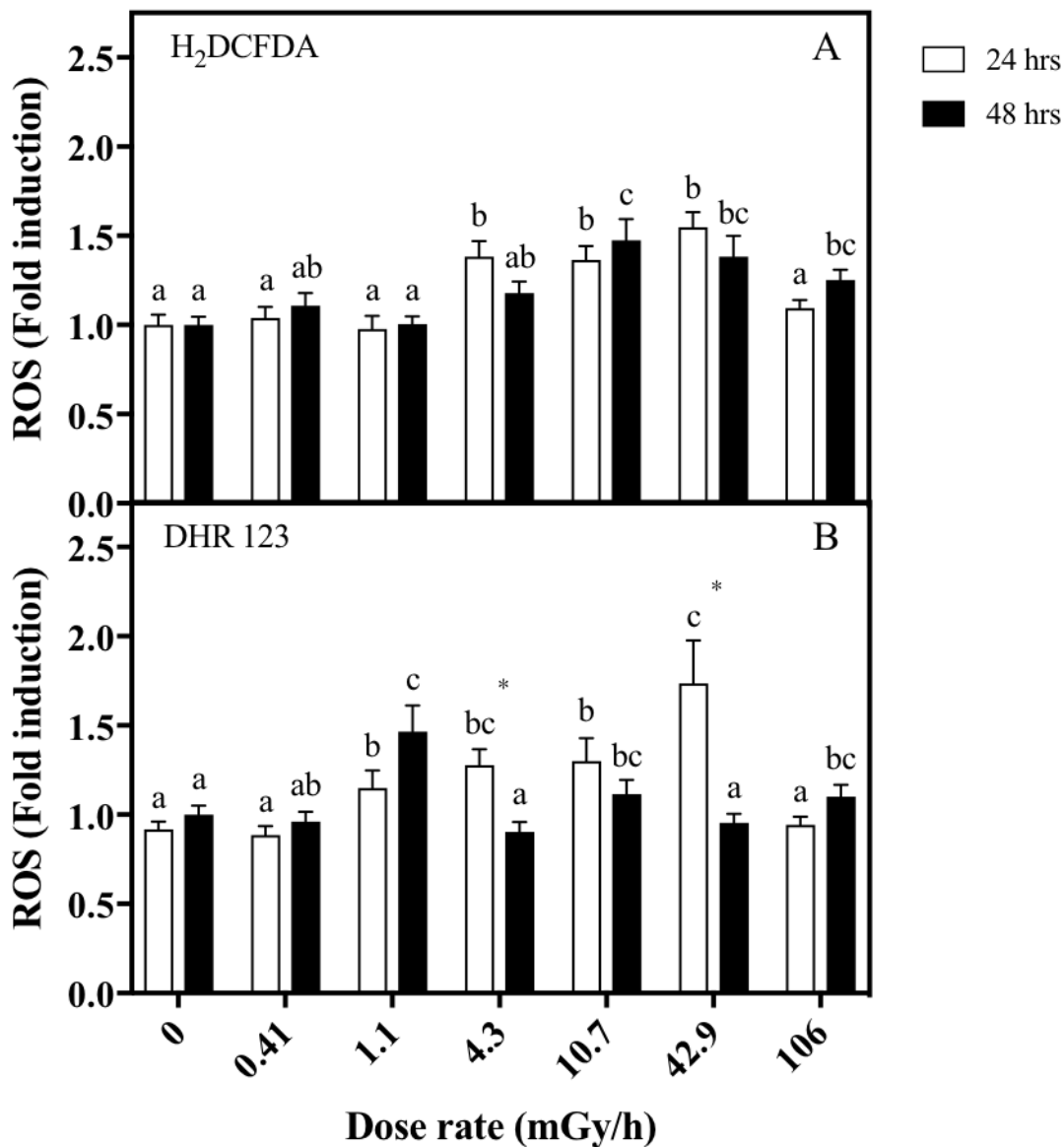
303 Following gamma radiation exposure (dose rates: 0.41, 1.1, 4.3, 10.7, 42.9 and 106 mGy/h), no  
304 significance difference in mortality, visual morphological or behavioural changes were  
305 observed between control and irradiated daphnia for all doses rates tested at 24 and 48 hrs. The  
306 temperature, pH and dissolved oxygen of the MHRW exposure media was  $20.0 \pm 0.05^{\circ}\text{C}$ ,  $8.1$   
307  $\pm 0.05$  and  $8.6 \pm 0.02$  mg/L during the exposure period, respectively.

308

#### 309 **3.2. ROS formation**

310 The formation of ROS was analysed regarding differences between dose rate and time of  
311 exposure using a two-way ANOVA (Supplementary Table A4). Results show that for the  
312 H<sub>2</sub>DCFDA fluorescence probe only the effect of dose rate was significant for the results  
313 obtained ( $p < 0.0001$ ), while for the DHR 123 probe, both time and dose rate were significant  
314 for the differences seen in exposed daphnids ( $p = 0.0384$  and  $p < 0.0001$ , respectively). Exposure  
315 to gamma radiation for 24 hrs caused a significant increase in ROS formation in *D. magna* at  
316 4.3 (1.4-fold), 10.7 (1.4-fold) and 42.9 mGy/h (1.5-fold), when measured by the H<sub>2</sub>DCFDA  
317 fluorescence probe (Figure 1A). Similar results were obtained with the DHR 123 probe (Figure  
318 1C), with significant ROS levels at dose rates higher than 1.1 mGy/h after 24 hrs exposure (up  
319 to a 1.7-fold increase at 42.9 mGy/h). The results obtained for both probes showed no  
320 significant ROS formation at the highest dose rate tested (106 mGy/h). After 48 hrs exposure,  
321 a significant increase in ROS formation was observed at 10.7 mGy/h and higher dose rates (up  
322 to 1.3-fold) in daphnids incubated with H<sub>2</sub>DCFDA (Figure 1B), even though no clear dose-  
323 response relationship was observed. In daphnids incubated with the DHR 123 probe, a  
324 significant increase in ROS formation was only detected at 1.1, 10.7 and 106 mGy/h ( $p < 0.05$ ),  
325 with a maximum 1.6-fold induction at 1.1 mGy/h (Figure 1D). Temporally, a decrease in ROS

326 formation from 24 to 48 hrs exposure was detected with DHR 124 only at 4.3 and 42.9 mGy/h  
 327 (Figure 1C-D).



328  
 329 **Figure 1** – Intracellular reactive oxygen species (ROS) formation measured by A) 2',7'-  
 330 dichlorodihydrofluorescein diacetate (H<sub>2</sub>DCFDA) and B) dihydrorhodamine 123 (DHR 123)  
 331 in *Daphnia magna* after 24 hrs and 48 hrs exposure to gamma radiation (average ± SEM).  
 332 Letters represent statistical differences between dose rates for each exposure period (p < 0.05).  
 333 Asterisk represent statistical differences between exposure period for each dose rate (p < 0.01).

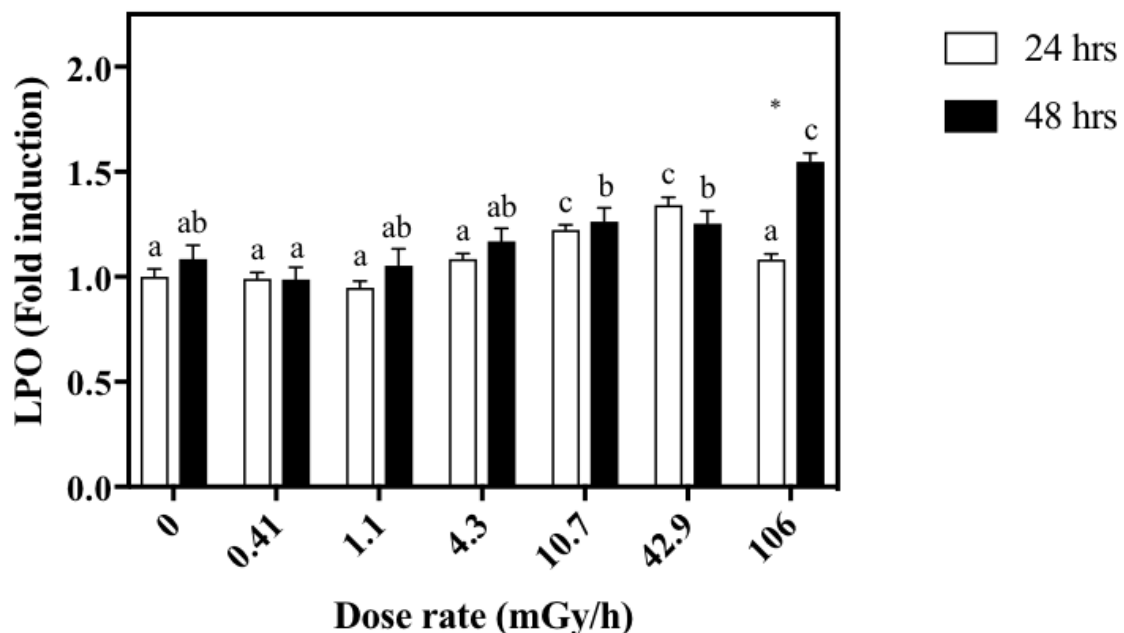
334

335 H<sub>2</sub>O<sub>2</sub> was used as a positive control to evaluate the performance of the ROS formation bioassay  
336 in *D. magna* using two fluorescent probes H<sub>2</sub>DFFDA and DHR 123. The results obtained  
337 showed a significant concentration dependent increase in ROS formation after 24 hrs exposure  
338 to H<sub>2</sub>O<sub>2</sub> (Supplementary Figure A1).

339

### 340 3.3. Lipid peroxidation

341 The two-way ANOVA showed that both time and dose rate had a significant effect on LPO  
342 data in exposed daphnids (Supplementary Table A4) and that their interaction was also  
343 significant ( $p < 0.0001$ ). Exposure to gamma radiation caused LPO in exposed daphnids after 24  
344 hrs exposure only at 10.7 and 42.9 mGy/h (1.2- and 1.3-fold, respectively, Figure 2A). After  
345 48 hrs exposure, a dose-dependent increase in LPO was detected (Figure 2B), reaching a 1.5-  
346 fold increase at the highest dose rate (106 mGy/h,  $p < 0.05$ ). A significant temporal increase in  
347 LPO was only detected at 106 mGy/h, with a 1.4-fold increase from 24 hrs to 48 hrs exposure.



348

349 **Figure 2** – Lipid peroxidation in *Daphnia magna* (5 to 6 groups of 36 pooled daphnids) was  
350 measured as malondialdehyde (MDA) and 4-hydroxyalkenals (4-HNE) after exposure to  
351 gamma radiation for 24 hrs and 48 hrs (average  $\pm$  SEM). Letters represent statistical differences

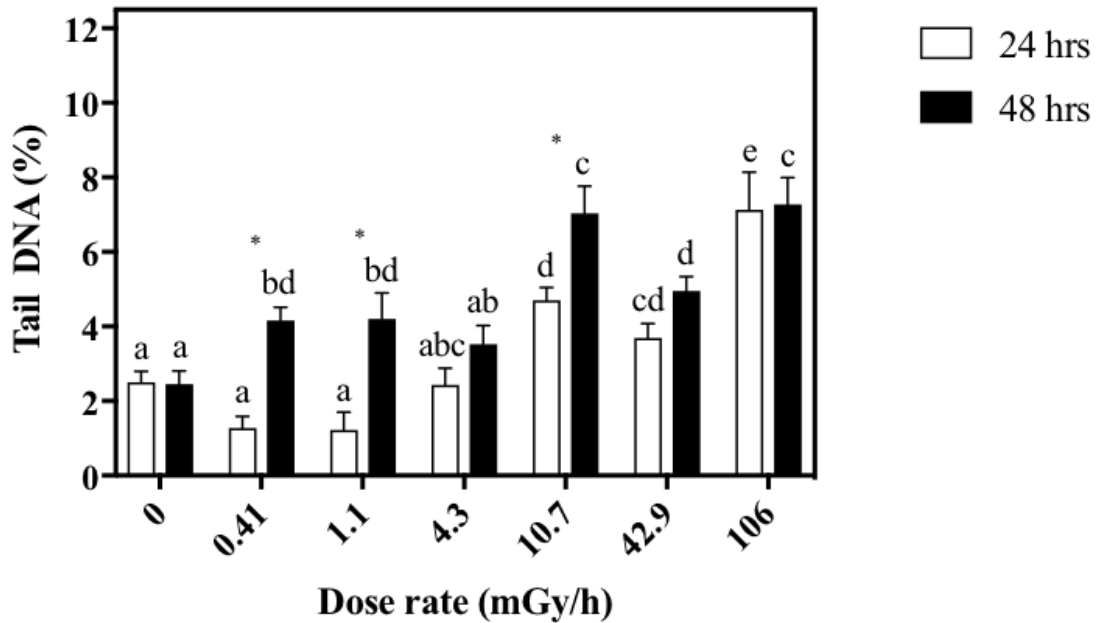


352 between dose rates for each exposure period ( $p<0.05$ ). Asterisk represent statistical differences  
353 between exposure period for each dose rate ( $p<0.0001$ ).

354

#### 355 **3.4. Comet assay**

356 Similarly to LPO, time and dose rate also had a significant effect on DNA damage  
357 (Supplementary Table A4) and that their interaction was also significant ( $p<0.0001$ ), as shown  
358 by the two-way ANOVA. Gamma radiation caused a small, but statistically significant increase  
359 in DNA-damage measured as single strand breaks (SSB) and alkali labile site formation in the  
360 haemolymph after 24 hrs of exposure at the highest doses (10.7, 42.9 and 106 mGy/h) compared  
361 to untreated controls. All dose rates except for 4.3 mGy/h caused DNA-damage after 48 hrs  
362 exposure. As for temporal variation, an increase in DNA-damage was observed at 0.41, 1.1 and  
363 10.7 mGy/h at 48 hrs exposure compared to 24 hrs. H<sub>2</sub>O<sub>2</sub> was used as a positive control and the  
364 results obtained showed a significant concentration-dependent increase in DNA damage in  
365 haemolymph from daphnids after 24 hrs, thus assuring a good quality control of the assay  
366 (Supplementary Figure A2). Cell viability was assessed using the trypan blue staining with cell  
367 viability >90 % at all dose rates used. Images of comets from haemolymph cells isolated from  
368 control and gamma radiation exposed daphnids are shown in Supplementary Figure A3.



369

370 **Figure 3** – DNA damage in *Daphnia magna* after exposure to gamma radiation for 24 hrs and  
 371 48 hrs (total 450 cells per dose rate, average  $\pm$  SEM). Letters represent statistical differences  
 372 between dose rates for each exposure period ( $p < 0.05$ ). Asterisk represent statistical differences  
 373 between exposure period for each dose rate ( $p < 0.001$ ).

374

### 375 **3.5. Global transcriptional alterations**

376 A massive number of transcriptional alterations were found in *D. magna* exposed 24 hrs to 42.9  
 377 and 106 mGy/h (3308 and 3352 DEGs, respectively), the highest dose rates tested, compared  
 378 to the intermediate dose rates of 1.1, 4.3 and 10.7 mGy/h (458, 534 and 1220 DEGs)  
 379 (Supplementary Table A5). Interestingly, exposure to the lowest gamma radiation dose rate of  
 380 0.41 mGy/h, resulted in a higher number of DEGs than the intermediate dose rates (2679  
 381 DEGs), suggesting a transcriptional response of *D. magna* also at low-dose rates  
 382 (Supplementary Table A5). The Venn diagram analysis (Supplementary Figure A4) revealed  
 383 that only 35 DEGs were identified to be common between all dose rates, whereas the majority  
 384 of transcriptional changes were due to up-regulation of the DEGs. The complete list of DEGs

385 that were regulated in *D. magna* after exposure to gamma radiation can be found in the  
386 Supplementary Table A6.

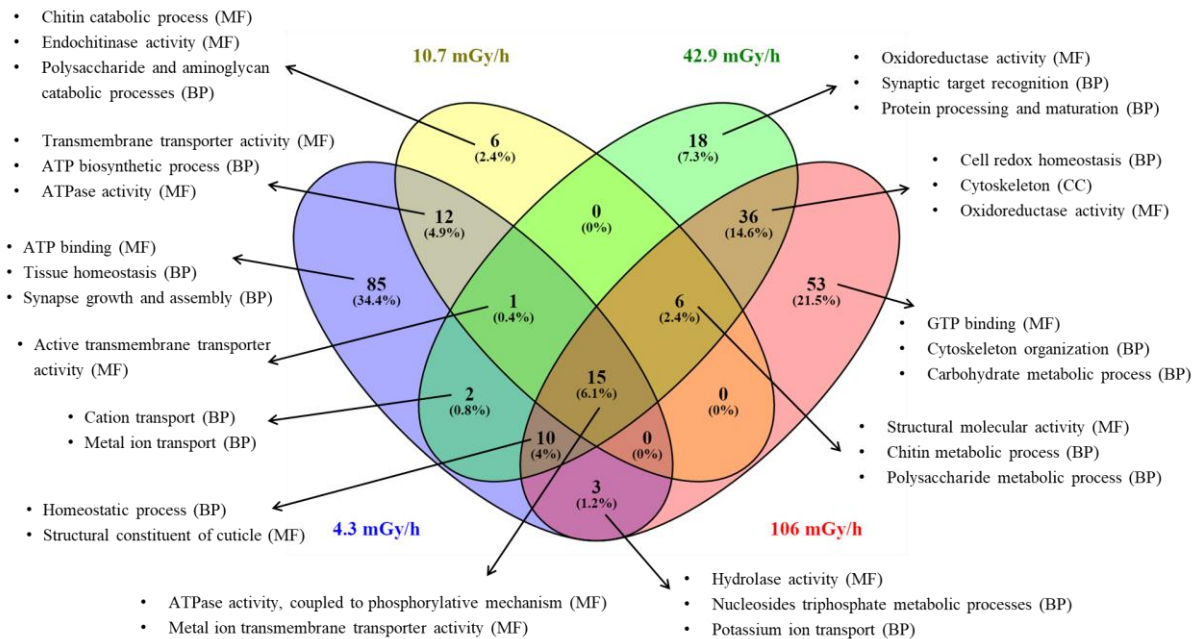
387

### 388 **3.6. Functional enrichment analysis**

389 Functional enrichment analysis showed that a total of 128, 40, 88 and 123 GO functions were  
390 over-represented after exposure to 4.3, 10.7, 42.9 and 106 mGy/h, with the majority being dose  
391 rate specific (Figure 4). No significant GO enrichment was identified at the two lowest dose  
392 rates tested (i.e., 0.41 and 1.1 mGy/h). Briefly, exposure to 4.3 mGy/h seems to modulate DEGs  
393 involved in ATP binding, tissue homeostasis, and synapse growth and assembly. Exposure to  
394 10.7 mGy/h resulted in the differential regulation of genes related to chitin catabolic process,  
395 endochitinase activity and polysaccharide and aminoglycan catabolic processes, while 42.9  
396 mGy/h regulated genes involved in oxidoreductase activity, synaptic target recognition and  
397 protein processing and maturing. The highest dose (106 mGy/h) regulated DEGs associated  
398 with GTP binding, cytoskeleton organization and carbohydrate metabolic process. Functions  
399 such as ATPase activity coupled to phosphorylative mechanism and metal ion transmembrane  
400 transporter activity were commonly regulated by all dose rates. The complete list of GO  
401 functions affected by the different dose rates used in this study can be found in the  
402 Supplementary Table A7.

403

404



405

406 **Figure 4** – Venn diagram analysis of overrepresented gene ontology (GO) functions that were  
 407 regulated in *Daphnia magna* after 24 hrs exposure to gamma radiation ( $p < 0.01$ ). A selection of  
 408 toxicologically relevant GO functions was identified and displayed. BP – Biological process,  
 409 MF – Molecular function, CC – Cellular component.

410

411 Pathway enrichment analysis further revealed a total of 73 (0.41 mGy/h), 6 (1.1 mGy/h), 11  
 412 (4.3 mGy/h), 37 (10.7 mGy/h), 119 (42.9 mGy/h) and 132 (106 mGy/h) pathways affected by  
 413 gamma radiation. Signal transduction, immune system and gene expression were identified as  
 414 the top functional categories with the most supporting pathways, while categories such as  
 415 transmembrane transport of small molecules (106 mGy/h) and DNA replication (42.9 mGy/h)  
 416 were only affected at specific dose rates (Supplementary Figure A5). Venn diagram analysis  
 417 allowed the identification of specific and common pathways affected by the different dose rates  
 418 (Supplementary Figure A6). In general, the higher number of pathways identified was at 106  
 419 mGy/h (e.g. G1/S DNA damage Checkpoints, p53-Independent DNA damage response, p53-  
 420 Independent G1/S DNA damage checkpoint, Ubiquitin mediated degradation of  
 421 phosphorylated Cdc25). The two highest dose rates tested displayed a higher number of

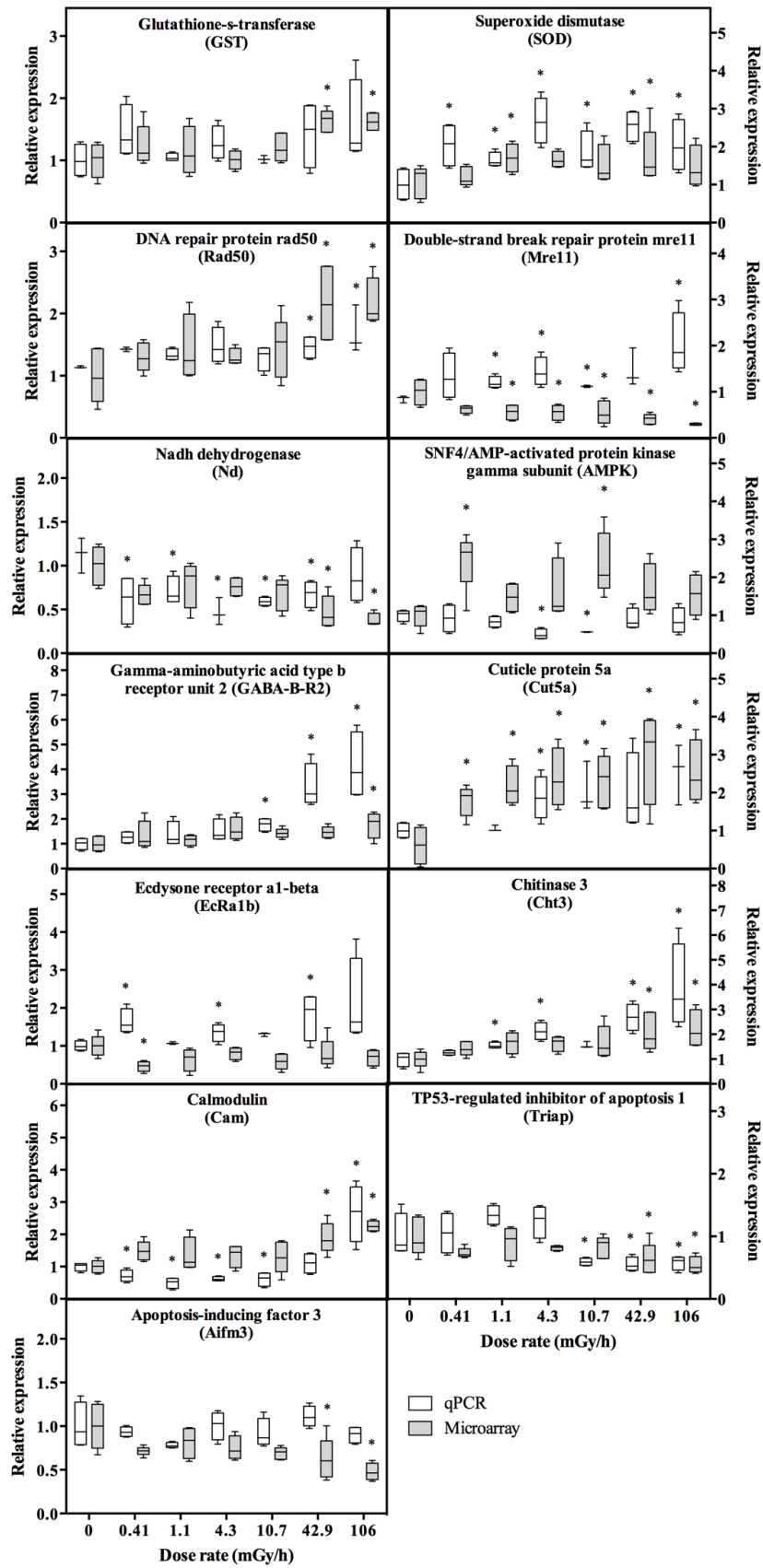
422 common pathways (total 58 pathways) than the remaining dose rates combined (e.g. calmodulin  
423 induced events, DNA damage/telomere stress induced senescence and GABA synthesis,  
424 release, reuptake and degradation). No pathway was commonly regulated across all dose rates.  
425 Pathways such as cell death signaling via NRAGE, NRIF and NADE, NRAGE signals death  
426 through JNK and P75 NTR receptor-mediated signaling were mainly affected by the lowest and  
427 highest dose rates used in this study (0.41 and 106 mGy/h), while pathways related to DNA  
428 double strand break response, recruitment and ATM-mediated phosphorylation of repair and  
429 signaling proteins at DNA double strand breaks were regulated by all dose rates except 1.1  
430 mGy/h. Several toxicologically relevant pathways and supporting DEGs representative of  
431 potential MoAs of gamma radiation were identified (Supplementary Table A8), such as DNA  
432 repair and cell cycle regulation, neurotransmitter signaling, mTOR signaling, oxidative stress  
433 and antioxidant defense, molting and developmental signaling, cell death, oxidative  
434 phosphorylation and calcium signaling. The complete list of pathways affected by the different  
435 dose rates used in this study can be found in the Supplementary Table A9.

436

### 437 **3.7. Quantitative real-time RT-PCR verification**

438 The expression of thirteen target genes involved in relevant toxicity pathways were verified by  
439 qPCR, namely glutathione s-transferase (*GST*), superoxide dismutase (*SOD*), DNA repair  
440 protein rad50 (*Rad50*), double-strand break repair protein mre11 (*Mre11*), NADH dehydrogenase  
441 (*Nd*), SNF4/AMP-activated protein kinase gamma subunit (*AMPK*), gamma-aminobutyric acid  
442 type b receptor subunit 2 (*GABA-B-R2*), cuticle protein5a (*Cut5a*), ecdysone receptor a1-beta  
443 (*EcRa1b*), chitinase 3 (*Cht3*), calmodulin (*Cam*), TP53-regulated inhibitor of apoptosis 1  
444 (*Triap*) and apoptosis-inducing factor 3 (*Aifm3*). The transcriptional patterns obtained by qPCR  
445 for the 13 target genes were in close agreement with those of the microarray (Fig. 5), with a  
446 general tendency of increased expression with increasing dose rate. The only exceptions were

447 the genes *Mre11* and *AMPK*, in which the patters obtained by the microarray were the opposite  
448 of those reflected by the qPCR. The similarity of transcriptional patterns obtained for the  
449 microarray and qPCR analyses was also evidenced by the significant correlation obtained for  
450 all genes ( $r=0.446$ ,  $p<0.0001$ ).



452 **Figure 5** – Gene response in *Daphnia magna* after 24h exposure to gamma radiation determined  
453 by quantitative real-time reverse transcription polymerase chain reaction (qPCR, white box,  
454 N=4-5) in comparison with microarray (grey box, N= 4-5). \*Represents significant statistical  
455 differences compared to the respective control ( $p<0.05$ ).

456

#### 457 **4. Discussion**

458 Even though aquatic ecosystems are continuously exposed to low levels of naturally occurring  
459 radionuclides, the anthropogenic inputs of man-made radionuclides in these ecosystems has  
460 increased the need to study their impact on aquatic organisms. These concerns have intensified  
461 especially after the Fukushima nuclear power plant accident in 2011, where large amounts of  
462 radioactive iodine and caesium were released into the surrounding aquatic environment,  
463 resulting in increasing concentrations in many aquatic species at dose rates above suggested  
464 benchmark levels (Buessler et al., 2012; Johansen et al., 2015; Nair et al., 2014). Nonetheless,  
465 there is still a lack of information about the toxic effects of ionizing radiation on invertebrate  
466 species, despite their essential role in aquatic ecosystems. In this context, this study aimed to  
467 understand the mechanism of toxicity of gamma radiation in the freshwater crustacean *D.*  
468 *magna* by identifying alterations in oxidative stress markers and their relation to alterations  
469 seen at the transcriptional level.

470 *D. magna* at the organismal level could tolerate gamma exposure up to 106 mGy/h for 48 hrs  
471 (total dose 5 Gy) without any sign of acute mortality, morbidity, or apparent developmental  
472 effects. No mortality, visual morphological or behavioural changes were detected in daphnids  
473 at any of the dose rates tested after the 48 hrs exposure to gamma radiation. This is in agreement  
474 with other studies, which have reported no effects in survival in *D. magna* as a result of acute  
475 exposure to gamma radiation generated by  $^{137}\text{Cs}$ , at doses higher than those used in this study  
476 (total doses from 2 to 28 Gy and 5 to 200 Gy) (Nascimento et al., 2015, 2016). In fact, the



477 estimated 50 % effect dose for mortality reported for gamma radiation ( $^{60}\text{Co}$  source) in *D.*  
478 *magna* after exposure is 1600 Gy and 1500 Gy for 24 and 48 hrs, respectively (Fuma et al.,  
479 2003). On the other hand, Sarapultseva and Dubrova (2016) observed a significant shortening  
480 in the life span of *D. magna* after acute exposure to  $^{60}\text{Co}$  (total doses of 100, 1000 and 10000  
481 mGy), nonetheless, these effects were observed 4 to 7 days following radiation exposure. Even  
482 though there were no significant effects in mortality in irradiated daphnia, the gamma radiation  
483 dose rates used in this study can be considered high, especially when compared to the suggested  
484 ecosystem screening benchmark of 0.24 mGy/h for the protection of freshwater ecosystems  
485 from radioactive substances (Garnier-Laplace et al., 2010). The total doses used are, however,  
486 within the range of those found in highly contaminated sites, such as reservoir at Mayak PA in  
487 Russia, used as waste ponds for decades, where the absorbed dose rates for zooplankton and  
488 phytoplankton were estimated as 3.8 and 40 Gy/day, respectively (Triapitsyna et al., 2012).  
489 Another example is the Techa River also at Mayak, where doses to biota have been estimated  
490 as high as 200-800 Gy after the accident in 1957 (Kryshev et al., 1998).

491

#### 492 **4.1. ROS formation**

493 Relative simple and rapid fluorescence assays for detecting ROS production have proven useful  
494 for the prediction of whole-organism toxicity, as previously seen in *D. magna* exposed to nano-  
495  $\text{TiO}_2$  under solar ultraviolet radiation (Ma et al., 2012). As anticipated, gamma radiation  
496 generated an apparent dose rate-dependent increase in ROS in daphnids after 24 h exposure (No  
497 Observed Effect Dose Rate, NOEDR of 1.1 mGy/h), particularly at dose rates higher than 1.1  
498 mGy/h. Interestingly, no significant ROS production was detected at the highest dose of 106  
499 mGy/h, as shown by both of the fluorescent probes. This lack of ROS formation can be  
500 potentially related to the combined protective action of radical scavenging antioxidants such as  
501 glutathione (GST), metallothionein and thioredoxin and/or induction of antioxidant enzymes

502 such as catalase (CAT), superoxide dismutase (SOD and glutathione-S-transferase (GST),  
503 among others (Reisz et al., 2014). This hypothesis is supported by the results obtained by  
504 transcriptional analysis which showed up-regulation of several antioxidant genes after 24 hrs  
505 exposure to gamma radiation at the highest dose rate. In fact, the *SOD* gene was up-regulated  
506 at all dose rates (qPCR) and at 1.1 and 42.9 mGy/h (microarray), suggesting that antioxidant  
507 enzymes were induced both at low and high dose rates. *GstS1* and *GstD5* were both up-  
508 regulated at the two highest dose rates (microarray), whereas no alterations were detected in  
509 *Gst* transcripts by qPCR. Thioredoxin peroxidase was also up-regulated at 0.41 mGy/h in  
510 addition to thioredoxin domain-containing protein at both 0.41 and 106 mGy/h. The induction  
511 of these antioxidant genes in *D. magna* after gamma radiation exposure confirms their central  
512 role in reducing oxidative stress caused by gamma radiation exposure at both low and high dose  
513 rates. Nonetheless, one cannot exclude the hypothesis that at intermediate dose rates, the  
514 antioxidant defence mechanisms triggered were insufficient to counterbalance the production  
515 of ROS, as seen at 42.9 mGy/h, or that other ROS-metabolizing molecules and detoxification  
516 enzymes not detected by the microarray analyses were affected. The induction of enzymatic  
517 and non-enzymatic antioxidants (SOD, CAT, GR (glutathione reductase), GPx (glutathione  
518 peroxidase), GST and GSH) has also been shown in other crustacean species (*Paracyclops*  
519 *nana*, *Tigriopus japonicus*, *Brachionus koreanus* and *Mesocyclops hyalinus*) in response to  
520 increased ROS production by gamma ( $^{137}\text{Cs}$  and  $^{60}\text{Co}$ ) radiation (Han et al., 2014a, b; Won and  
521 Lee, 2014). After 48 hrs of exposure to gamma radiation, a dose-dependent ROS formation was  
522 observed in irradiated daphnids with a NOEDR of 1.1 mGy/h, similarly to what was seen at 24  
523 hrs. In contrast to the response at 24 hrs, a significant ROS production was detected at 106  
524 mGy/h after 48 hrs exposure, which may reflect temporal activation of direct ROS formation  
525 and activation of intracellular ROS-producing systems (e.g. mitochondria) at high doses (Reisz  
526 et al., 2014). Although the present study is the first to document gamma radiation-induced ROS

527 in *D. magna*, it has been documented for other aquatic invertebrates elsewhere (see review by  
528 Won et al., 2014).

529

#### 530 **4.2. Lipid peroxidation**

531 Excessive ROS formation can induce oxidative stress and cause damage to lipids, proteins and  
532 DNA thus disturbing normal cellular functions (Reisz et al., 2014). Lipid peroxidation in  
533 particular, is characterized by the oxidative deterioration of polyunsaturated fatty acids present  
534 in cellular membranes, which can result in membrane destabilization and further oxidative  
535 damage (Halliwell and Gutteridge, 2007). Results from the present study verify that exposure  
536 to gamma radiation increased LPO at 10.7 and 42.9 mGy/h (24 and 48 hrs) when measured as  
537 MDA and 4-HNE, which were consistent with the observations on ROS formation at the same  
538 dose rates and exposure period. At 106 mGy/h, an increase in LPO was only observed after 48  
539 hrs exposure, thus suggesting that the antioxidant protective system was capable of limiting  
540 oxidative damage only at lower dose rates and shorter exposure times. At the remaining dose  
541 rates, the production of ROS apparently exceeded the antioxidant capacity of cells. Nonetheless,  
542 the hypothesis that the rate of ROS produced at 10.7 and 42.9 mGy/h were not high enough to  
543 trigger the antioxidant defence mechanisms and counteract their oxidative damage cannot be  
544 excluded as a possible explanation for the LPO levels seen in irradiated daphnids. Although  
545 this is the first study to report gamma radiation-induced LPO formation in invertebrates,  
546 disruption of the integrity of membranous lipid bilayers in mammalian cells (Azzam et al.,  
547 2012) and plants (Jan et al., 2012) suggest that LPO may be a conserved MoA of gamma  
548 radiation across species.

549

#### 550 **4.3. DNA damage**

551 The genotoxicity measured as increase in DNA of haemocytes from *D. magna* by the Comet  
552 assay suggest that gamma radiation caused significant decrease in DNA integrity, especially at  
553 the highest dose rates. Although this increase was small and variable along the dose rates tested,  
554 an overall dose rate-response relationship resembling that of ROS and LPO was observed. It's  
555 well established that radiation induced-ROS attack DNA, generating a variety of DNA lesions,  
556 such as oxidized bases and strand breaks (single and double DNA strand breaks). If not properly  
557 removed, DNA damage by direct interaction and enhanced ROS formation by radiation can  
558 accumulate to the point where it leads to mutagenesis (Maynard et al. 2009). Ionizing radiation  
559 can lead to a broad spectrum of DNA lesions (Goodhead, 1989), including increased incision  
560 in the backbone of DNA while repairing. Since the damage persisted in exposed daphnids for  
561 48 hrs, it may suggest that induction of DNA repair capacity was not sufficiently effective to  
562 counteract the damage caused by ionizing radiation in haemolymph cells. It has been suggested  
563 that low doses of radiation may not activate DNA repair, thus leading to recovery processes  
564 being triggered only above a critical level of damage. This may result in the elimination of the  
565 damaged cells by apoptosis or mitotic death (Hayes 2008; Zaichkina et al., 2004) and possibly  
566 a selection of less damaged cells is analysed at low dose rates. Radiation-induced DNA damage  
567 has been previously reported in *D. magna* exposed to <sup>137</sup>Cs source (Parisot et al., 2015). In this  
568 case, an overall accumulation and transmission of DNA alterations was registered across three  
569 successive *D. magna* generations in a time and dose-dependent manner, at dose rates from  
570 0.0007 to 35.4 mGy/h. These authors hypothesized that DNA repair mechanisms become  
571 efficient only after organisms receive a sufficient cumulative dose of radiation, especially under  
572 chronic exposure (Parisot et al., 2015). Dose-dependent modulation of genes such as DNA-PK,  
573 PCNA, Ku70 and Ku80, involved in DNA repair in the rotifer *B. koreanus* and the copepods *T.*  
574 *japonicus* and *P. nana*, suggest that exposure to <sup>137</sup>Cs (total doses from 10 to 200 Gy) also cause  
575 DNA damage in other invertebrates (Han et al., 2014a, b; Won and Lee, 2014). In the present

576 study, several DEGs and pathways related to DNA repair and cell cycle regulation were affected  
577 by gamma radiation, probably as a consequence of handling destabilized and damaged DNA.  
578 From the several DEGs identified herein, the up-regulation of DNA repair proteins rad 50  
579 (*Rad50*) (42.9 and 106 mGy/h) and MRE11-like (*mre11*) (1.1, 4.3, 10.7 and 106 mGy/h),  
580 constituents of a repair complex implicated in multiple DNA repair mechanisms (Brodsky et  
581 al., 2004), confirm that daphnids repairing systems responded effectively to exposure to gamma  
582 radiation, initiating a recovery of cellular damages especially at higher dose rates. *mre11*  
583 seemed to be more responsive than *Rad50* at low dose rates, albeit inconsistencies between the  
584 microarray and qPCR data for *mre11* suggest that additional effort is required to characterize  
585 the transcription regulation of this gene in *D. magna* in response to gamma radiation.

586

#### 587 **4.4. Energy production and homeostasis**

588 Another important cellular target of ionizing radiation and consequent ROS formation is the  
589 mitochondria. Gamma radiation has been associated with mitochondrial dysfunction in the form  
590 of mitochondria-dependent ROS formation, increased mitochondrial membrane potential and  
591 promoted respiration and ATP production (Kam and Banati, 2013; Reisz et al., 2014), processes  
592 that can lead to further propagation of ROS and oxidative stress. In the present study, several  
593 genes related to the mitochondria were differentially regulated in daphnids exposed to gamma  
594 radiation. Several DEGs involved in mitochondrial electron transport chain (ETC) were  
595 suppressed by gamma radiation, namely genes encoding NADH dehydrogenase (*Nd*) in  
596 complex I, succinate dehydrogenase subunit A (*SdhA*) in complex II, cytochrome c oxidase  
597 subunit 1 (*COX1*), cytochrome c oxidase subunit 2 (*COX2*), cytochrome c oxidase subunit 3  
598 (*COX3*) and cytochrome c oxidase copper chaperone (*COX17*) in complex IV, and ATP  
599 synthase subunit mitochondrial (*sun*) in complex V. Only the gene encoding succinate  
600 dehydrogenase B (*SdhB*) in complex II was induced by gamma radiation (0.41, 42.9 and 106

601 mGy/h). No DEGs involved in ETC complex III were differentially regulated in the irradiated  
602 daphnia. The *Nd* gene was also found to be significantly down-regulated by qPCR at 4.1, 1.1,  
603 4.3 10.7 and 42.9 mGy/h, even though the microarray analysis only showed significant  
604 suppression at the two highest dose rates used. These results suggest that gamma radiation may  
605 interfere with mitochondrial membrane function in daphnids, modulate oxidative  
606 phosphorylation (OXPHOS) and ultimately cause loss of aerobic energy supply or even cell  
607 death (Joshi and Bakowska, 2011). The reduction of mitochondrial membrane potential and  
608 associated ATP synthesis in response to gamma radiation has been documented in several  
609 mammalian and fish species (Kam and Banati, 2013, O'Dowd et al., 2006, Song et al., 2014),  
610 although the knowledge of the MoA in crustaceans is still limited.

611 A potential imbalance of energy homeostasis in daphnids exposed to gamma radiation was also  
612 evidenced by the enrichment of a pathway involved in the mechanistic target of rapamycin  
613 (mTOR) signaling. In vertebrate species, alterations in cellular energy balance impact mTOR  
614 signaling via AMPK, a Serine Threonine kinase consisting of a catalytic  $\alpha$ -subunit and two  
615 regulatory subunits,  $\beta$  and  $\gamma$  (Huang and Fingar, 2014; Roux and Topisirovic, 2012). In the  
616 present study, the SNF4/AMP-activated protein kinase gamma subunit (*SNF4Agamma*) gene  
617 was induced (microarray analysis) in irradiated daphnia probably due to an alteration in the  
618 intracellular AMP/ATP ratio associated with mitochondrial dysfunction (Lippai et al., 2008).  
619 This result was the opposite of that found by qPCR, in which the *SNF4Agamma* gene was down-  
620 regulated at 4.3 and 10.7 mGy/h. The inhibition of the mTOR signaling pathway can also  
621 stimulate autophagy due to a rise in free cytosolic calcium, as well as the stimulation of the  
622 lipid mechanism (Huang and Fingar, 2014). A dysregulation of mTOR as a possible mechanism  
623 of radiotoxicity has already been reported in zebrafish embryos exposed to the same gamma  
624 source as that used in this study (Hurem et al., 2017), however its function in irradiated *D.*  
625 *magna* needs to be further explored.

626

#### 627 **4.5. Cell death**

628 Apoptosis has been extensively documented in cells upon exposure to gamma radiation,  
629 normally as a consequence of oxidative stress and associated cell cycle arrest, DNA damage,  
630 impairment of DNA repair and mitochondrial dysfunction (Reisz et al., 2014). Several genes  
631 involved in the modulation of several apoptotic pathways were significantly regulated by  
632 gamma radiation. For example, the down-regulation of apoptosis-inducing factor 3 (*Aifm*,  
633 microarray: 42.9 and 106 mGy/h) and p53-regulated inhibitor of apoptosis 1 (*Triap*, qPCR:  
634 10.7, 42.9 and 106 mGy/h), two genes involved in the modulation of the mitochondrial  
635 apoptotic pathway, is suggestive of a potential induction of apoptosis, however, not through  
636 major signaling pathways. In addition, the enrichment of pathways related to neuronal cell death  
637 was also identified in *D. magna* after exposure to 0.41 and 106 mGy/h, highlighting the onset  
638 of cognitive dysfunction in daphnids following radiation exposure. Taken together, results  
639 suggest that different apoptotic signaling pathways were regulated in daphnids in response to  
640 gamma radiation, which seems to be consistent with the identified DNA damage and repair,  
641 cell cycle disruption, mitochondrial dysfunction and neurotransmission impairment. The  
642 induction of apoptosis after exposure to the same gamma source as that used in this study has  
643 already been documented in fish, namely Atlantic salmon and zebrafish, in which the regulation  
644 of different apoptotic signaling was also highlighted in response to upstream mechanisms as for  
645 example oxidative stress and DNA damage and repair (Song et al., 2014, Hurem et al., 2017).

646

#### 647 **4.6. Ca<sup>2+</sup> homeostasis and other potential mechanisms**

648 The gene pathway analysis highlighted other potential MoA of gamma radiation in daphnids.  
649 A general activation of genes associated with Calcium signaling pathways such as Ca-  
650 dependent events, Calmodulin induced events and CaM pathway were observed in daphnids

651 exposed to 42.9 and 106 mGy/h. Calmodulin (*CaM*), the ubiquitously expressed and highly  
652 conserved protein that is essential for numerous cellular processes and is the key mediator of  
653  $\text{Ca}^{2+}$  signals (Altshuler et al., 2015; Song et al., 2016), was significantly down-regulated by  
654 0.41, 1.1, 4.3 and 10.7 mGy/h and up-regulated at 106 mGy/h (qPCR). Cells tightly regulate  
655 their cytoplasmic calcium concentrations, as  $\text{Ca}^{2+}$  ions are used in a several concentration-  
656 dependent processes, which in crustaceans can be directly related to molting, mTOR signaling  
657 and intracellular calcium influx (Altshuler et al., 2015). Accordingly, these results seem to point  
658 to a dose rate-dependent disruption in  $\text{Ca}^{2+}$  homeostasis by gamma radiation, which may play  
659 an important role in the activation/suppression of several processes in *D. magna*, as for example  
660 mitochondrial dysfunction, mTOR signaling, neurochemical signaling and endocrine  
661 regulation.

662 Exposure to gamma radiation also affected the neurochemical signaling system in exposed  
663 daphnids, as neuronal system-related pathways were significantly enriched at the two highest  
664 dose rates used (42.9 and 106 mGy/h). Among these, pathways related to glutamate and GABA  
665 signaling were identified as the most significant, as highlighted by the up-regulation of the  
666 gamma-aminobutyric acid type b receptor subunit 2-like (*GABA-B-R2*) gene by both the  
667 microarray (106 mGy/h) and qPCR (10.7, 42.9 and 106 mGy/h) analysis at the highest dose  
668 rates used. GABA-mediated signaling has been extensively studied in crustacean species due  
669 to its role in synaptic transmission and neural inhibition (Northcutt et al., 2016), as well as its  
670 involvement in the regulation of cell development (Salat and Kulig, 2011). Even though no  
671 studies have focused on the neurotransmitter related-effects of gamma radiation in crustaceans,  
672 there is evidence that the modulation of these pathways is related to cognitive dysfunction  
673 following radiation exposure in mammals (see Wu et al., 2012 and references herein).  
674 Nonetheless, the molecular mechanisms underlying the up- and downstream signaling of these  
675 pathways in response to gamma radiation still remain to be elucidated in *D. magna*.



676 Another novel finding in the present study was that multiple genes associated with the endocrine  
677 regulation of molting in *D. magna* were differentially expressed after exposure to gamma  
678 radiation. These transcriptional alterations suggest that as low as 0.41 mGy/h gamma may  
679 disrupt molting signaling by inhibiting the synthesis of ecdysteroids, thus potentially leading to  
680 suppressed transcriptional regulation of molting through the EcR. Inhibition of ecdysteroid  
681 synthesis may be attributed by increased intracellular calcium influx, which has been shown to  
682 suppress ecdysteroid synthesis in crustaceans (Chang and Mykles, 2011). On the contrary, high  
683 dose-rate of gamma potentially induced the expression of cuticle proteins, which are necessary  
684 for the generation of new exoskeletons in *D. magna* (Song et al., 2017). Two examples of the  
685 effects of gamma radiation in daphnids exoskeleton is the significant induction of genes  
686 encoding for the cuticle protein 5a (*Cut5a*) and chitinase 3 (*Cht3*) at both low and high dose  
687 rates, as shown by both the microarray and qPCR analysis. However, whether these molecular  
688 responses can lead to impaired molting at the organismal still needs to be verified.

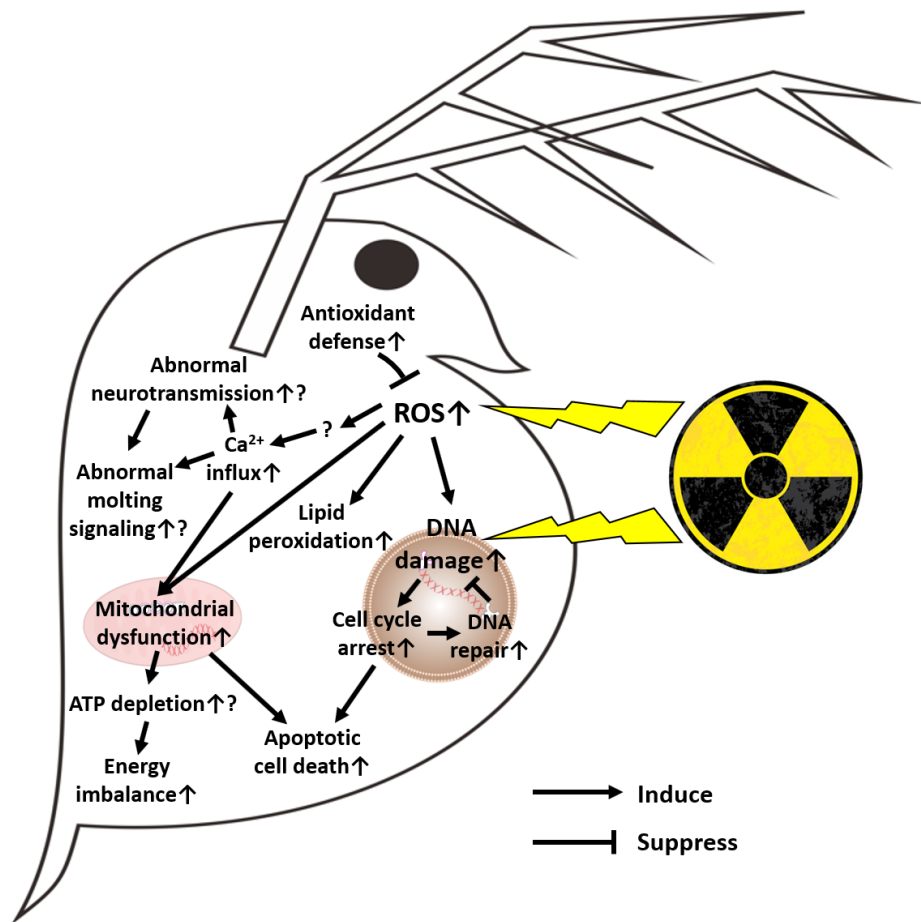
689

## 690 **5. Conclusions**

691 The present study showed that acute exposure to gamma radiation resulted in significant  
692 alterations at the cellular and molecular level in the crustacean *D. magna*. Results showed a  
693 significant dose and time-dependent increase in ROS formation in daphnids, which is consistent  
694 with the MoA of gamma radiation in cells. Moreover, the LPO and DNA damage observed in  
695 gamma-irradiated daphnids showed dose rate and cumulative dose and time dependent effects,  
696 which seems to be connected not only to oxidative stress, but also to radiolysis mechanisms.  
697 Transcriptional analysis further highlighted oxidative stress as one of the main MoA of gamma  
698 radiation, especially at high dose rates, suggesting a strong causal relationship between cellular  
699 and molecular disturbances upon gamma radiation exposure. This include the induction of  
700 oxidative damages to DNA and lipids through excessive ROS formation, as well as causing

701 mitochondrial ETC dysfunctions and cellular energy imbalance, possibly through direct  
702 damage to the mitochondrial membranes by ROS and/or as a result of potentially increased  
703 calcium influx to the mitochondria. Additional toxicological relevant MoAs were evidenced by  
704 microarray analysis, further suggesting that downstream responses such as antioxidant defense,  
705 cell cycle regulation and DNA repair, apoptotic cell death, abnormal neurotransmission and  
706 disruption of molting signaling may also be affected. However, since no adverse effects were  
707 observed due to the short exposure duration, whether these were adaptive (compensatory)  
708 responses or toxicity pathways leading to adversity still need to be investigated. Further  
709 assessment using relevant functional endpoints are also necessary to help understand the  
710 mechanistic link between these molecular alterations and organism level responses. In addition,  
711 it still remains to be verified if the alterations observed are also relevant at lower dose rates,  
712 including a purported low dose-rate effect at 0.41 mGy/h, and if the dose rates used in this study  
713 are sufficient to induce cumulative effects in daphnids at longer and more environmentally  
714 relevant exposure durations, as well as over a range of successive generations. Overall, the  
715 results obtained allowed the identification of a suite of biomarker genes associated with several  
716 biological mechanisms that could be used in future evaluation of toxicity and MoA of ionizing  
717 radiation in *D. magna*. Accordingly, based on both functional and transcriptional responses  
718 observed in irradiated *D. magna*, several putative MoAs for gamma radiation are thus proposed  
719 (Figure 6).

720



721

722 **Figure 6** – Putative toxicity mechanisms of gamma radiation in *Daphnia magna*.

723

724 **Conflict of interest**

725 The authors declare the inexistence of any conflict of interest.

726

727 **Acknowledgements**

728 This work was supported by the Research Council of Norway through its Centres of Excellence  
 729 funding scheme, project number 223268/F50. The authors would like to thank Ole Christian  
 730 Lind and Yetneberk A. Kassaye for their help with the radiation experiments and to Ann-Karin  
 731 Olsen for the laboratory resources.

732

733 **5. References**

734 Altshuler, I., McLeod, A.M., Colbourne, J.K., Yan, N.D., Cristescu, M.E., 2015. Synergistic  
735 interactions of biotic and abiotic environmental stressors on gene expression. *Genome* 58, 99–  
736 109.

737 Azzam, E.I., Jay-Gerin, J.-P., Pain, D., 2012. Ionizing radiation-induced metabolic oxidative  
738 stress and prolonged cell injury. *Cancer let.* 327(0), 48-60.

739 Bindea, G., Mlecnik, B., Hackl, H., Charoentong, P., Tosolini, M., Kirilovsky, A., Fridman, W.  
740 H., Pages, F., Trajanoski, Z., Galon, J., 2009. ClueGO: A Cytoscape plug-in to decipher  
741 functionally grouped gene ontology and pathway annotation networks. *Bioinformatics.* 25,  
742 1091–1093.

743 Bjerke, H., Hetland, P.O., 2014. Dosimetri ved FIGARO gammaanlegget ved NMBU, Ås.  
744 Målerapport fra oppmåling av doseraten i strålefeltet fra kobolt-60. NRPA Technical Document  
745 Series 2.

746 Bradford, M.M., 1976. A rapid and sensitive method for the quantitation of microgram  
747 quantities of protein utilizing the principle of protein-dye binding. *Anal. Biochem.* 72, 248–  
748 254.

749 Brodsky, M., Weinert, B.T., Tsang, G. Rong, Y.S., McGinnis, N.M., Golic, K.G., Rio, D.C.  
750 Rubin, G.M., 2004. *Drosophila melanogaster* MNK/Chk2 and p53 Regulate Multiple DNA  
751 Repair and Apoptotic Pathways following DNA Damage. *Mol. Cel. Biol.* 24(3), 1219–1231

752 Buessler, K.O., Jayne, S.R., Fisher, N.S., Rypina, I.I., Baumann, H., Baumann, Z., Yoshida,  
753 S., 2012. Fukushima-derived radionuclides in the ocean and biota off Japan. *Proc. Natl. Acad.*  
754 *Sci.* 109 (16), 5984–5988.

755 Chang, E.S., Mykles, D.L., 2011. Regulation of crustacean molting: a review and our  
756 perspectives. *Gen. Comp. Endocrinol.* 172(3), 323-30.

757 Dallas, L.J., Keith-Roach, M., Lyons, B.P., Jha, A.N., 2012. Assessing the impact of ionizing  
758 radiation on aquatic invertebrates: a critical review. *Rad. Res.* 177, 693-716.

759 Erdelmeier, I., Gérard-Monnier, D., Yadan, J.-C., Chaudière, J., 1998. Reactions of N-methyl-  
760 2-phenylindole with malondialdehyde and 4-hydroxyalkenals. Mechanistic aspects of the  
761 colorimetric assay of lipid peroxidation. *Chem. Res. Toxicol.* 11, 1184–1194.

762 Fuller, N., Lerebours, A., Smith, J.T., Ford, A.T., 2015. The biological effects of ionising  
763 radiation on Crustaceans: A review. *Aquat. Toxicol.* 167, 55-67.

764 Fuma, S., Ishii, N., Tanaka, N., Takeda, H., Miyamoto, K., Yanagisawa, K., Saito, M.,  
765 Ichimasa, Y., 2003. Comparative evaluation of the effects of  $\gamma$ -rays and heavy metals on  
766 mobility of the water flea *Daphnia magna*. *Radioisotopes.* 52, 319-326.

767 Garnier-Laplace, J., Della-Vedova, C., Andersson, P., Copplestone, D., Cailes, C., Beresford,  
768 N.A., Howard, B.J., Howe, P., Whitehouse, P., 2010. A multi-criteria weight of evidence  
769 approach for deriving ecological benchmarks for radioactive substances. *J. Radiol. Prot.* 30,  
770 215–233.

771 Gilbin, R., Alonzo, F., Garnier-Laplace, J., 2008. Effects of chronic external gamma irradiation  
772 on growth and reproductive success of *Daphnia magna*. *J. Environ. Radioactiv.* 99, 134-145.

773 Goodhead, D.T., 1989. The initial physical damage produced by ionizing radiations, *Int. J.*  
774 *Radiat. Biol.* 56, 623–634.

775 Gutzkow, K.B., Langleite, T.M., Meier, S., Graupner, A., Collins, A.R., Brunborg, G., 2013.  
776 High-throughput comet assay using 96 minigels. *Mutagenesis* 28, 333–340.

777 Halliwell, B., Gutteridge, J.M.C., 2007. *Free Radicals in Biology and Medicine*, fourth ed.  
778 Oxford University Press, New York.

779 Han, J., Won, E.-J., Kim, I.-C., Yim, J.H., Lee, S.-J., Lee, J.-S., 2014. Sublethal gamma  
780 irradiation affects reproductive impairment and elevates antioxidant enzyme and DNA repair  
781 activities in the monogonont rotifer *Brachionus koreanus*. *Aquat. Toxicol.* 155, 101-109.

782 Han, J., Won, E.-j., Lee, B.-Y., Hwang, U.-K., Kim, I.-C., Yim, J.H., Leung, K.M.Y., Lee, Y.S.,  
783 Lee, J.-S., 2014. Gamma rays induce DNA damage and oxidative stress associated with

784 impaired growth and reproduction in the copepod *Tigriopus japonicus*. *Aquat. Toxicol.* 152,  
785 264-272.

786 Hansen, E.L., Hetland P.O., 2015. Air kerma measurements with Landauer nanoDots in Cs-137  
787 and Co-60 beams, Part I - SSDL reference exposures free in air. NRPA Technical Document  
788 Series 8.

789 Hayes, D.P., 2008. Non-problematic risks from low-dose radiation-induced DNA damage  
790 clusters. *Dose Response.* 6(1), 30–52.

791 Huang, K., Fingar, D.C., 2014. Growing knowledge of the mTOR signaling network. *Semin.*  
792 *Cell. Dev. Biol.* 36, 79-90.

793 Hurem, S., Martín, L.M., Brede, D.A., Skjerve, E., Nourizadeh-Lillabadi, R., Lind, O.C.,  
794 Christensen, T., Berg, V., Teien, H.-C., Salbu, B., Oughton, D.H., Aleström, P., Lyche, J.L.,  
795 2017. Dose-dependent effects of gamma radiation on the early zebrafish development and gene  
796 expression. *Plos One.* 12(6), e0179259.

797 ICRP 2008. Environmental Protection - the Concept and Use of Reference Animals and Plants.  
798 ICRP Publ. 108 Ann. 38 (4-6).

799 Jan, S., Parween, T., Siddiqi, T.O., Mohmooduzzafar, 2012. Effect of gamma radiation on  
800 morphological, biochemical, and physiological aspects of plants and plant products. *Environ.*  
801 *Rev.* 20, 17-39.

802 Jensen, L.K., Halvorsen, E., Song, Y., Hallanger, I.G., Hansen, E.L., Brooks, S.J., Hansen,  
803 B.H., Tollefsen, K.E., 2016. Individual and molecular level effects of produced water  
804 contaminants on nauplii and adult females of *Calanus finmarchicus*. *J. Toxicol. Environ. Health*  
805 *A* 79, 585-601.

806 Johansen, M.P., Ruedig, E., Tagami, K., Uchida, S., Higley, K., Beresford, N.A., 2015.  
807 Radiological dose rates to marine fish from the Fukushima Daiichi accident: the first three years  
808 across the North Pacific. *Environ. Sci. Technol.* 49, 1277e1285.

809 Joshi, D.C., Bakowska, J.C., 2011. Determination of mitochondrial membrane potential and  
810 reactive oxygen species in live rat cortical neurons. *J. Vis. Exp.* 23,7588–7596.

811 Kam, W.W., Banati, R.B., 2013. Effects of ionizing radiation on mitochondria. *Free Radic.*  
812 *Biol. Med.* 65, 607–619.

813 Kim, H.J., Koedrith, P., Seo, R. Y., 2015. Ecotoxicogenomic approaches for understanding  
814 molecular mechanisms of environmental chemical toxicity using aquatic invertebrate, *Daphnia*  
815 model organism. *Int. J. Mol. Sci.* 16, 12261-12287.

816 Kryshev, I.I., Romanov, G.N., Sazykina, T.G., Isaeva, L.N., Trabalka, J.R., Blaylock, B.G.,  
817 1998. Environmental contamination and assessment of doses from radiation releases in the  
818 Southern Urals. *Health Phys.* 74, 687e697.

819 Kumaravel, T.S., Jha, A.N., 2006. Reliable Comet assay measurements for detecting DNA  
820 damage induced by ionising radiation and chemicals. *Mutat. Res. Toxicol. Environ. Mutagen.*  
821 605, 7–16.

822 Lippai, M., Csikós, G., Maróy, P., Lukácsovich, T., Juhász, G., Sass, M., 2008. SNF4A $\gamma$ , the  
823 *Drosophila* AMPK  $\gamma$  subunit is required for regulation of developmental and stress-induced  
824 autophagy, *Autophagy*, 4:4, 476-486.

825 Ma, H., Brennan, A., Diamond, S.A., 2012. Photocatalytic reactive oxygen species production  
826 and phototoxicity of titanium dioxide nanoparticles are dependent on the solar ultraviolet  
827 radiation spectrum. *Environ. Toxicol. Chem.* 31(9), 2099-2107.

828 Maere, S., Heymans, K., and Kuiper, M., 2005. BiNGO: A Cytoscape plugin to assess  
829 overrepresentation of gene ontology categories in biological networks. *Bioinformatics.* 21,  
830 3448–3449.

831 Marshall, J.S., 1966. Population dynamics of *Daphnia pulex* as modified by chronic radiation  
832 stress. *Ecology.* 47(4), 561-571.

833 Marshall, J.S.,1962. The effects of continuous gamma radiation on the intrinsic rate of natural  
834 increase of *Daphnia pulex*. Ecology. 43(4), 598-607.

835 Maynard, S., Schurman, S.H., Harboe, C., de Souza-Pinto, N.C., Bohr, V.A., 2009. Base  
836 excision repair of oxidative DNA damage and association with cancer and aging.  
837 Carcinogenesis. 30(1):2-10.

838 Nair, R.N., Sunny, F., Chopra, M., Sharma, L.K., 2014. Estimation of radioactive leakages into  
839 the Pacific Ocean due to Fukushima nuclear accident. Environ. Earth Sci. 71(3), 1007-1009.

840 Nascimento, F.J.A., Svendsen, C., Bradshaw, C., 2015. Combined effects from  $\gamma$  radiation and  
841 fluoranthene exposure on carbon transfer from phytoplankton to zooplankton. Env. Sci.  
842 Technol. 49, 10624-10631.

843 Nascimento, F.J.A., Svendsen, C., Bradshaw, C., 2016. Joint toxicity of cadmium and ionizing  
844 radiation on zooplankton carbon incorporation, growth and mobility. Env. Sci. Technol. 50,  
845 1527-1535.

846 Nascimento, J.A., Bradshaw, C., 2016. Direct and indirect effects of ionizing radiation on  
847 grazer-phytoplankton interactions. J. Environ. Radioactiv. 155-156, 63-70.

848 Northcutt, A.J., Let, K.M., Garcia, V.B., Diester, C.M., Lane, B.J., Marder, E., Schulz, D.J.,  
849 2016. Deep sequencing of transcriptomes from the nervous system of two decapod crustaceans  
850 to characterize genes important for neural circuit function and modulation. BMC Genomics.  
851 17, 868.

852 O'Dowd, C., Mothersill, C.E., Cairns, M.T., Austin, B., McClean, B., Lyng, F.M., Murphy,  
853 J.E., 2006. The release of bystander factor(s) from tissue explant cultures of rainbow trout  
854 (*Onchorhynchus mykiss*) after exposure to gamma radiation. Radiat. Res. 166, 611–617.

855 OECD, 2004. OECD guidelines for testing of chemicals. Guideline 202: *Daphnia* sp., acute  
856 immobilisation test.



857 OECD, 2008. OECD guidelines for testing of chemicals. Guideline 211: *Daphnia magna*  
858 reproduction test.

859 Parisot, F., Bourdineaud, J.-P., Plaire, D., Adam-Guillermin, C., Alonzo, F., 2015. DNA  
860 alterations and effects on growth and reproduction in *Daphnia magna* during chronic exposure  
861 to gamma radiation over three successive generations. *Aquat. Toxicol.* 163, 27-36.

862 Pellegrini, V., Gorbi, G., Buschini, A., 2014. Comet assay on *Daphnia magna* in eco-genotoxicity  
863 testing. *Aquat. Toxicol.* 155, 261-268.

864 Pfaffl, M.W., 2001. A new mathematical model for relative quantification in real-time RT-  
865 PCR, *Nucleic Acids Research*, 29, e45-e45.

866 Reisz, J.A., Bansal, N., Qian, J., Zhao, W., Furdai, C.M., 2014. Effects of ionizing radiation on  
867 biological molecules – Mechanisms of damage and emerging methods of detection. *Antioxid.*  
868 *Redox Sig.* 21(2), 260–291.

869 Roux, P.P., Topisirovic, I., 2012. Regulation of mRNA translation by signaling pathways. *Cold*  
870 *Spring Harb. Perspect. Biol.* 4, a012252.

871 Salat, K., Kulig, K., 2011. GABA transporters as targets for new drugs. *Future Med. Chem.*  
872 3(2), 211-222.

873 Sarapultseva, E., Uskalova, D., Savina, N., Ustenko, K., 2017. Medical-biological aspects of  
874 radiation effects in *Daphnia magna*. *IOP Conf. Series: Journal of Physics: Conf. Series.* 784,  
875 012052.

876 Sarapultseva, E.I., Dubrova, Y.E., 2016. The long-term effects of acute exposure to ionising  
877 radiation on survival and fertility in *Daphnia magna*. *Environ. Res.* 150, 138-143.

878 Sarapultseva, E.I., Gorski, A.I., 2013. Low-dose  $\gamma$ -irradiation affects the survival of exposed  
879 daphnia and their offspring. *Dose-Response.* 11, 460-468.

880 Shaw, J.R., Pfrender, M.E., Eads, B.D., Klaper, R., Callaghan, A., Colson, I., Jansen, B.,  
881 Gilbert, D., Colbourne, J.K., 2008. *Daphnia* as an emerging model for toxicological genomics.

882 In Hogstrand, C. and Kille, P., editors, *Comparative Toxicogenomics*, 2, Advances in  
883 Experimental Biology, chapter 6, pages 165–220. Elsevier, Oxford.

884 Smoot, M.E., Ono, K., Ruscheinski, J., Wang, P.L., Ideker, T., 2011. Cytoscape 2.8: New  
885 features for data integration and network visualization. *Bioinformatics*. 27: 431–432.

886 Smyth, G.K., 2005. Limma: Linear models for microarray data. In *Bioinformatics and*  
887 *computational biology solutions using R and Bioconductor*, ed. R. Gentleman, V.J. Carey, W.  
888 Huber, R.A. Irizarry, and S. Dudoit, 397–420. New York, NY: Springer.

889 Song, Y., Salbu, B., Teien, H.-C., Heier, L.S., Rosseland, B.O., Tollefsen, K.E., 2014. Dose-  
890 dependent hepatic transcriptional responses in Atlantic salmon (*Salmo salar*) exposed to  
891 sublethal doses of gamma radiation. *Aquat. Toxicol.* 156, 52-64.

892 Song, Y., Villeneuve, D.L., Toyota, K., Iguchi, T., Tollefsen, K.E., 2017. Ecdysone receptor  
893 agonism leading to lethal molting disruption in arthropods: review and adverse outcome  
894 pathway development. *Environ. Sci. Technol.* 51(8), 4142-4157.

895 Song, Y., Rundberget, J.T., Evenseth, L.M., Xie, L., Gomes, T., Høgåsen, T., Iguchi,  
896 T., Tollefsen, K.E., 2016. Whole-organism transcriptomic analysis provides mechanistic  
897 insight into the acute toxicity of emamectin benzoate in *Daphnia magna*. *Environ. Sci.*  
898 *Technol.* 50(21): 11994-12003.

899 Triapitsyna, G.A., Andreev, S.S., Osipov, D.I., Stukalov, P.M., Ivanov, I.A., Aleksandrova,  
900 O.N., Kostiuchenko, A.V., Priakhin, E.A., Akleev, A.V., 2012. Assessment of radiation  
901 exposure level for hydrobionts in some special industrial ponds at the “Mayak” PA. *Radiats*  
902 *Biol. Radioecol.* 52, 207e214.

903 United States Environmental Protection Agency. 1996. Ecological Effects Test Guidelines  
904 OPPTS 850.1300 Daphnid Chronic Toxicity Test. US EPA, 12p.

905 UNSCEAR 2008. Sources and effects of ionizing radiation. Report to the General Assembly,  
906 with scientific annex. New York, United Nations: UNSCEAR – United Nations Scientific  
907 Committee on the Effects of Atomic Radiation, 2010.

908 Ward, J.F., 1995. Radiation mutagenesis: the initial DNA lesions responsible. *Radiat. Res.* 142,  
909 362-368.

910 Watanabe, H., Kobayashi, K., Kato, Y., Oda, S., Abe, R., Tatarazako, N., Iguchi, T., 2008.  
911 Transcriptome profiling in crustaceans as a tool for ecotoxicogenomics. *Cell Biol. Toxicol.* 24,  
912 641-647.

913 Won, E.-J., Dahms, H.-U., Kumar, K.S., Shin, K.-H., Lee, J.-S., 2014. An integrated view of  
914 gamma radiation effects on marine fauna. *Environ. Sci. Pollut. Res.* 22(22), 17443-17452.

915 Won, E.-J., Lee, J.-S., 2014. Gamma radiation induces growth retardation, impaired egg  
916 production, and oxidative stress in the marine copepod *Paracyclops nana*. *Aquat. Toxicol.*  
917 150, 17-26.

918 Wu, P.H., Coultrap, S., Pinnix, C., Davies, K.D., Taylor, R., Ang, K.K., Browning, M.D.,  
919 Grosshans, D.R., 2012. Radiation induces acute alterations in neuronal function. *Plos One.* 7(5),  
920 e37677.

921 Xie, F., Lampi, M.A., Dixon, D.G., Greenberg, B.M., 2007. Assessment of the toxicity of  
922 mixtures of nickel or cadmium with 9,10-phenanthrenequinone to *Daphnia magna*: impact of  
923 a reactive oxygen-mediated mechanism with different redox-active metals. *Environ. Toxicol.*  
924 *Chem.* 26(7), 1425-1432.

925 Zaichkina, S., Rozanova, O., Aptikaeva, G., Achmadieva, A.C., Klovov, D., 2004. Low doses  
926 of gamma radiation induce nonlinear dose responses in mammalian and plant cells. *Nonlinear.*  
927 *Biol. Toxicol. Med.* 2, 213–221.